

## Enhancement of Single-Molecule Fluorescence Detection in Subwavelength Apertures

Hervé Rigneault,<sup>1,\*</sup> Jérémie Capoulade,<sup>1</sup> José Dintinger,<sup>2</sup> Jérôme Wenger,<sup>1</sup> Nicolas Bonod,<sup>1</sup> Evgeni Popov,<sup>1</sup> Thomas W. Ebbesen,<sup>2</sup> and Pierre-François Lenne<sup>1,†</sup>

<sup>1</sup>Institut Fresnel, Domaine Universitaire de Saint Jérôme, Université d'Aix-Marseille III, CNRS UMR 6133, 13397 Marseille Cedex 20, France

<sup>2</sup>ISIS, Université Louis Pasteur, CNRS UMR 7006, 8 allée G. Monge, 67000 Strasbourg, France

(Received 9 December 2004; published 6 September 2005)

We report the experimental proof of molecular count rate enhancement (up to 6.5-fold) and lifetime reduction for single fluorescent molecules diffusing in subwavelength apertures milled in aluminum films. The observed enhancement dependence with the aperture diameter agrees qualitatively with numerical electromagnetic computations of the excitation power density into the aperture volume.

DOI: 10.1103/PhysRevLett.95.117401

PACS numbers: 78.67.-n, 32.50.+d, 81.07.-b, 82.37.Vb

In any single-molecule experiment, the weak fluorescence signal needs to be discriminated against the background. A strategy consists in enhancing the spontaneous emission by tailoring the electromagnetic environment the molecule can radiate into [1,2]. In principle, both the emission rate and the angular radiation pattern can be affected, and these fundamental effects have been investigated at the single-molecule level in near field optics experiments where a metal coated tip aperture is scanned above a fixed fluorescent molecule [3,4]. The influence of nanometric photonics structures to enhance single emitters radiation has recently gained interest since the observation of the enhanced fluorescence by a sharp metal tip [5] or nanometric particles in Raman scattering [6]. Much work has also been motivated by the discovery of the enhanced transmission phenomena where surface plasmons give rise to strong electromagnetic fields at the entrance of subwavelength apertures [7]. Of particular interest are isolated single holes (possibly surrounded by corrugated surfaces) where localized surface plasmon modes are involved [8,9] to enhance the transmission of light.

Fluorescence correlation spectroscopy (FCS) may offer new applications to characterize the use of nanophotonics devices. FCS is a well-known and powerful technique to study single-molecule fluorescence properties [10], where the fluctuations are analyzed by autocorrelating temporally the recorded photocount signal  $n(t)$ . This is quantified by the fluctuation autocorrelation function (ACF),  $g^{(2)}(\tau) = \frac{\langle n(t)n(t+\tau) \rangle}{\langle n(t) \rangle^2}$  where  $\langle \rangle$  stands for an ensemble averaging. Recently, Levene *et al.* [11] investigated for the first time the diffusion dynamics of single molecules in nanometric metallic apertures using FCS. In this work, tiny subwavelength holes (diameter  $d < 80$  nm) were milled in aluminum films and were shown to act as small reaction chambers with an effective observation volume  $V_{\text{eff}}$  down to  $10^{-21}$  l, allowing one to study chemical reactions at molecular concentrations up to 0.2 mM. Although no alteration of the spontaneous emission was reported in [11], a subwavelength aperture containing few molecular emitters is very similar to the near field optics experi-

ments where drastic alteration of the spontaneous emission has been observed [3,4]. However, the tiny aperture diameter used in [11] may have prevented Levene and his co-workers from observing any alteration of the molecular fluorescence.

In this Letter, we investigate the potential of single nanometric apertures milled in metal films to enhance the photocount rate per molecule  $\eta$  in FCS experiments. This is performed by studying apertures with a diameter between 110 and 420 nm, thus significantly larger than in [11]. Using isolated single holes, we report a striking 6.5-fold enhancement of  $\eta$  as compared to free solution together with a significant decrease of the observation volume  $V_{\text{eff}}$  for small hole diameters. The fluorescence enhancement is associated with a dramatic reduction of the molecular lifetime, which demonstrates that the energy levels' branching ratios are affected for molecules located in subwavelength apertures. A fundamental point reported here is that the metal nanoaperture allows one, on one hand, to postpone the fluorescence saturation by affecting the molecular branching ratios, while, on the other hand, the local excitation intensity is increased by the aperture, thus yielding a net fluorescence rate per molecule significantly higher as compared to open solution. Numerical electromagnetic simulations using the differen-

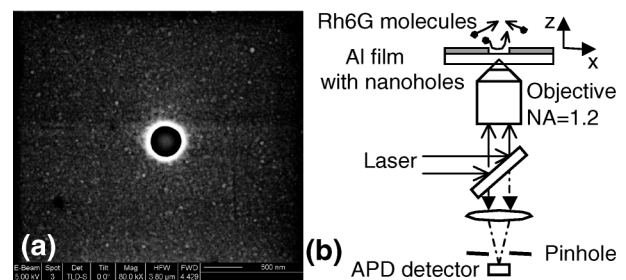


FIG. 1. (a) Scanning electron micrograph of an isolated subwavelength aperture milled in an Al film coated on a microscope slip. (b) Schematic view of the optical setup (APD: avalanche photodiode).

tial theory are implemented and give predictions consistent with our observations.

Optically thick Al metal films (thickness  $h = 300$  nm) were coated on conventional microscope slips (thickness  $150 \mu\text{m}$ ) by thermal evaporation. Subwavelength apertures (diameter  $d$  from 110 to 420 nm) were fabricated by focused ion beam (FEI Strata DB235 using  $\text{Ga}^+$  ions exhibiting a 5 nm nominal beam diameter). Figure 1 shows the scanning electron micrograph of such an aperture. FCS experiments were performed in a custom setup based on an inverted microscope (Zeiss Axiovert 200) with an NA = 1.2 objective lens (Zeiss C-Apochromat). Nanopositioning of the aperture was possible thanks to a multi-axis piezostage (Physik Instrumente P527). ACFs were recorded by a hardware correlator (ALV 6000) and fitted with IgorPro software (WAVEMETRICS). We used as fluorescent reporters Rhodamine 6G molecules (Rh6G) with an excitation wavelength of 488 nm provided by an argon ion laser (Fig. 1). Tight focusing conditions were used to shine a single subwavelength aperture with a beam waist of 250 nm (calibrated from FCS experiments carried out on Rh6G in solution). This setup provides an observation volume  $V_{\text{eff}}$  of 750 attoliters. For the experiments reported here, the laser polarization was set linear. The incoming power was kept below 1 mW at the back microscope lens aperture to avoid the sample damage. Two photons fluorescence lifetime of Rh6G was recorded by a time-to-amplitude converter (TimeHarp-PicoQuant) following a 4 MHz ps pulses train provided by a pulsed picked mode locked Ti:sapphire laser tuned at a wavelength of 800 nm.

Figure 2 presents the measured evolution of  $V_{\text{eff}}$  with the subwavelength aperture diameter  $d$ . Knowing the molecular concentration, the observation volume is deduced from the mean number of molecules  $N$  that is obtained from

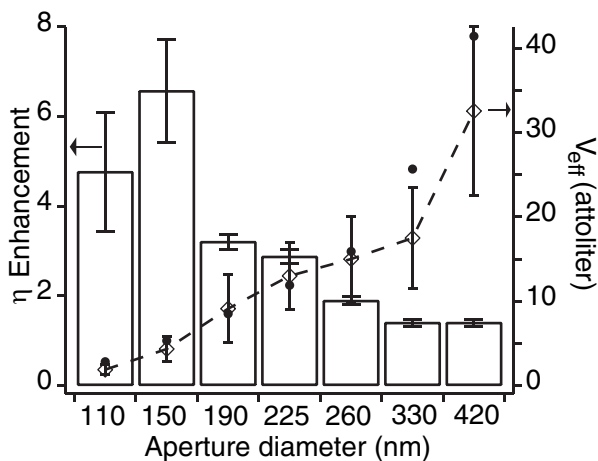


FIG. 2.  $V_{\text{eff}}$  evolution versus the aperture diameter ( $\diamond$ , right scale—dashed line to guide the eyes) and nanohole geometrical volume ( $\bullet$ , right scale). Enhancement of  $\eta$  (histogram, left scale) as compared to its value in open solution versus the aperture diameter ( $P_{\text{ex}} = 0.2$  mW).

$g^{(2)}(0) = 1 + \frac{1}{N} \left(1 - \frac{\langle b \rangle}{\langle i \rangle}\right)^2 (1 + n_T)$  where  $\langle i \rangle$  is the mean intensity,  $\langle b \rangle$  the mean background, and  $n_T$  the triplet amplitude related to the fraction  $F$  of molecules in the triplet state by  $F = n_T / (1 + n_T)$ . Let us point out that this expression of  $g^{(2)}(0)$  is independent of the shape of the excitation field and the type of molecular diffusion, and its validity holds for a stationary system and a dilute solution where the spatial correlation length of concentration fluctuations is much smaller than the detection volume [12]. For each experimental run, the triplet amplitude  $n_T$  was fitted to the raw experimental ACFs (assuming a free 3D diffusion; see Fig. 3). For instance, with an excitation power of  $300 \mu\text{W}$ ,  $n_T$  was found in the range  $n_T = 0.35 \pm 0.15$  for the various nanohole diameters. The background noise  $b$  within the apertures was recorded with a nanohole filled with pure water [see the photocount trace and the  $g^{(2)}(\tau)$  for the noise in Fig. 3].  $b$  does not exhibit any time correlation. A clear reduction of  $V_{\text{eff}}$  is observed, which is always equal to or smaller than the geometrical nanohole volume ( $\pi d^2 h / 4$ ), suggesting that the electromagnetic fields involved in the FCS process are essentially limited to this volume. The 110 nm diameter aperture exhibits a  $V_{\text{eff}}$  of 1.8 attoliters enabling single-molecule detection for concentrations in the  $\mu\text{M}$  range. This volume reduction is associated with the reduction of the diffusion time across  $V_{\text{eff}}$  as illustrated by the ACF functions presented in Fig. 3, which are recorded in open solution and into a  $d = 150$  nm

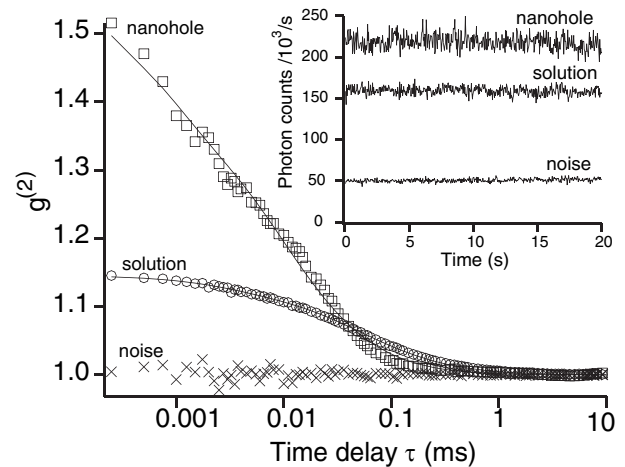


FIG. 3. Line traces and autocorrelation functions in open solution ( $\circ$ ) in a 150 nm diameter aperture ( $\square$ ) and for the noise within the aperture ( $\times$ ) for an excitation power of 0.3 mW (the noise was negligible in open solution:  $< 200$  counts/s). The molecular concentration for the experiment in open solution was set to 20 nM, while it was taken to 600 nM within the aperture. For the open solution, numerical fits assuming a 3D free diffusion yield the set of parameters:  $N = 7.8$ ,  $n_T = 0.15$ , diffusion time is  $53 \mu\text{s}$ , count rate per molecule is 20 kHz. For the 150 nm aperture,  $N = 1.5$ ,  $n_T = 0.35$ , diffusion time is  $10 \mu\text{s}$ , count rate per molecule is 112 kHz.

aperture. We found that this diffusion time reduction is consistent with the measured  $V_{\text{eff}}$  shown in Fig. 2.

To study the ability of these nanostructures to alter single-molecule fluorescence detection, we investigated the evolution of the detected count rate per molecule  $\eta$  with the aperture diameter. This information is readily obtained in FCS measurements by dividing the photon counted signal by the number of molecules  $N$  present in  $V_{\text{eff}}$  computed from  $g^{(2)}(0)$ . Figure 2 presents the enhancement of  $\eta$  as compared to its value in open solution for an excitation laser power  $P_{\text{ex}} = 0.2$  mW, at which the fluorescence is in the linear regime for FCS experiments carried out in the nanohole or in free solution. A significant enhancement is observed for the small holes' diameters ( $<200$  nm) although a twofold enhancement is commonly seen for aperture diameters in the 250–400 nm range. Figure 4 shows the evolution of  $\eta$  with the excitation laser power in a 150 nm diameter aperture and in open solution. In the linear regime ( $P_{\text{ex}} < 0.4$  mW),  $\eta$  was found up to  $\sim 6.5$  times stronger for the molecule diffusing within the subwavelength apertures as compared to open solution. For  $P_{\text{ex}} > 0.4$  mW,  $\eta$  saturates to  $\sim 30$  kHz for Rh6G molecules in open solution, whereas the linear regime persists in nanoholes up to  $P_{\text{ex}} \sim 1$  mW. Let us emphasize that since Rh6G is a high quantum efficiency dye, the triplet amplitude  $n_T$  remains quite small while increasing the excitation power. By fitting the experimental data for each excitation power, we found that  $n_T$  increased slowly with typically  $n_T = 0.25$  at  $150 \mu\text{W}$  and  $n_T = 0.5$  at  $900 \mu\text{W}$  for a 150 nm nanohole. We confirmed that no bleaching processes were involved in the saturation curve in open solution or in the nanoholes as the diffusion time and the

number of molecule remain constant with increasing power. A striking  $\eta$  of 350 kHz was recorded into the 150 nm aperture for  $P_{\text{ex}} = 1$  mW, in this case the apparent enhancement reaches 12.

To get insight into the radiative processes involved in this fluorescence enhancement, we investigated the molecular excited state lifetime inside the nanoholes as compared to open solution. The inset of Fig. 4 shows the fluorescence radiative decay curve in open solution and into a  $d = 150$  nm aperture. A striking reduction from 3.7 ns in open solution down to our apparatus response time (0.9 ns) is observed in good agreement with the previously observed lifetime reduction at the rim of the metallic tip in near field optics [13,14]. This shows that the molecular energy levels branching ratios are affected for dye molecules diffusing in nanoholes as compared to open solution, allowing for a delay of the fluorescence saturation inside the subwavelength apertures. Although nonradiative processes due to the metal surface must be involved in the observed lifetime reduction, the enhancement of  $\eta$  demonstrates that the overall effect acts in favor of the radiative processes as compared to open solution. In addition to the possible alteration of the intersystem branching ratio, a coupling between the molecule and plasmon resonances may also increase the radiative rate.

Several physical arguments can contribute to the observed enhancement, which can be simply written as  $\eta = \frac{1}{N} \int \text{CEF}(r) I_{\text{ex}}(r) dr$ , where  $N$  is the FCS mean number of molecules present in  $V_{\text{eff}}$ ,  $I_{\text{ex}}(r)$  is the local excitation intensity, and  $\text{CEF}(r)$  stands for the local collection efficiency function [15]. This expression is valid when no saturation occurs. Note that  $\text{CEF}(r)$  stands for the electromagnetic power emitted by a dipole located at  $\mathbf{r}$ , which is collected by the detector; in this respect, it includes the radiation pattern alteration and the possible lifetime reduction. Both the  $\text{CEF}(r)$  and  $I_{\text{ex}}(r)$  are expected to be affected by the metallic subwavelength aperture boundary conditions as compared to open solution [16]. The observed  $\eta$  enhancement cannot be solely due to an increase of  $I_{\text{ex}}(r)$  because otherwise one would expect the fluorescence to saturate as in open solution, without yielding any supplementary photocount. On the other hand, an alteration of the molecular radiation pattern collection could increase  $\text{CEF}(r)$  only by, at most, a factor of 3.3 since the objective microscope lens already collects 30% of the emitted light in open solution. In this case the saturation would be expected at  $30 \times 3.3 \sim 100$  kHz in nanoholes. Because of the dramatic fluorescence lifetime reduction inside the nanohole, we conclude that the molecular energy levels' branching ratios are affected, leading to a delay in the fluorescence saturation.

The complete description of the process would require the calculation of the  $\text{CEF}(r)$  and is beyond the scope of this paper. We rather focus here on the role played by the excitation field  $I_{\text{ex}}(r)$  on  $\eta$ . We therefore made the assump-

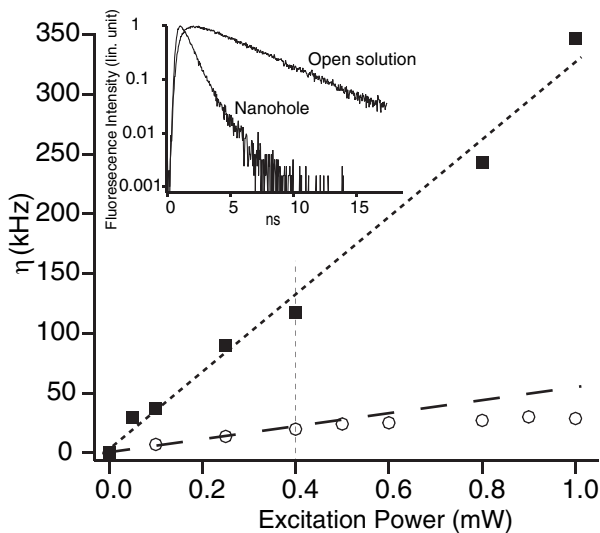


FIG. 4. Evolution of  $\eta$  versus the incident power  $P_{\text{ex}}$  in a 150 nm aperture (■) and in open free solution (○). Inset: Fluorescence decay curves in open solution and into a  $d = 150$  nm nanohole.

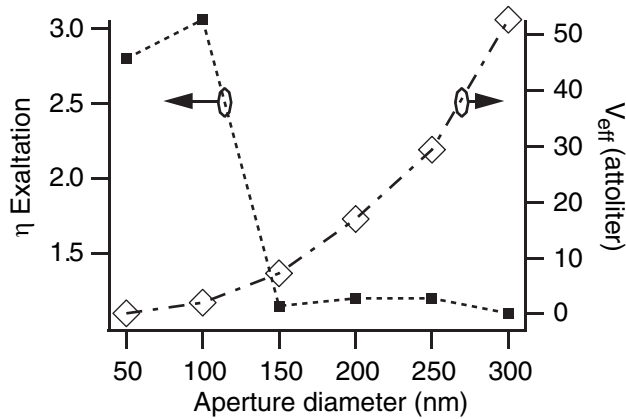


FIG. 5. Results of simulations in a 200 nm thick metal film. Count rate per molecule  $\eta$  (normalized to the open solution case) and effective volume  $V_{\text{eff}}$  as a function of the aperture diameter.

tion that  $\text{CEF}(r) = 1$  to compute  $\eta$  and the effective FCS volume [15] defined in this case as  $V_{\text{eff}} = \frac{(\int I_{\text{ex}}(r)dr)^2}{\int I_{\text{ex}}^2(r)dr}$ . To perform such calculations in a single circular hole drilled in a plane metallic sheet, we use the generalized differential theory that we have recently developed to study diffractive structures described in cylindrical coordinates [17,18]. Figure 5 presents the computed evolution of  $\eta$  (normalized to open solution) and  $V_{\text{eff}}$  with the aperture diameter. Numerical convergence constraints [17,18] make impossible the modelling of very highly conducting metals and, we have used material with lower conductivity. In order to preserve almost the same decay depth of the field in the aperture, the calculation were performed with a collimated beam incoming on a 200 nm thick metal layer with and  $\epsilon = -8 + i3$ , which is different from the real case ( $h = 300$  nm and  $\epsilon_{\text{AL}} = -30 + i7$ ). Despite this difference and the  $\text{CEF}(r) = 1$  assumption, we observe a clear reduction of  $V_{\text{eff}}$ . The striking feature is the enhancement of  $\eta$  for the small diameter apertures (around 100 nm). Numerical results indicate that this behavior is related to the field enhancement, which takes place at the edge of the nanohole [9,19,20]. This field enhancement is due to the plasmon excitation and is localized close to the holes' edges. When compared to the total aperture surface, the region of the enhanced field is relatively larger for smaller apertures than for larger ones, thus leading to an enhancement of  $\eta$ . For very small diameters ( $<100$  nm), the field penetrates at a very small depth inside the hole, and this edge effect becomes less important.

These numerical simulations are qualitatively consistent with our experimental observations. Nevertheless, the 6.5-fold enhancement of  $\eta$  experimentally observed is not explained and requires a deeper investigation of the radia-

tion pattern and the lifetime changes of a source located inside a nanohole.

In conclusion, we have investigated by FCS the fluorescence of individual molecules diffusing in subwavelength apertures milled in aluminum films. Besides the reduction of the observation volume, we report a significant enhancement of the count rate per molecule for small aperture diameters. Because the fluorescence lifetime is dramatically reduced in nanohole, we conclude that the molecular energy levels' branching ratios are affected leading to a delay in the fluorescence saturation. The combination of this effect together with an increase in the local excitation intensity induced by the metal aperture yields an overall fluorescence enhancement as compared to open solution. The experimental observations are qualitatively confirmed by electromagnetic calculations of the excitation field density inside the aperture. By taking benefit of this significant enhancement, such apertures could serve as efficient nano-optical sources or nanowells for fast and highly parallel molecular analysis at high concentration.

The authors are grateful to J. M. Gérard and M. Nevrière for stimulating discussions and M. Cathelinaud for the realization of the aluminum coatings. This work was funded by the "ACI Nanosciences" of the Research French Ministry.

\*Electronic address: herve.rigneault@fresnel.fr

†Electronic address: lenne@fresnel.fr

- [1] E. M. Purcell, Phys. Rev. **69**, 681 (1946).
- [2] K. H. Drexhage, Prog. Opt. **12**, 163 (1974).
- [3] X. S. Xie and R. C. Dunn, Science **265**, 361 (1994).
- [4] H. Gersen *et al.*, Phys. Rev. Lett. **85**, 5312 (2000).
- [5] E. J. Sánchez, L. Novotny, and X. S. Xie, Phys. Rev. Lett. **82**, 4014 (1999).
- [6] S. Nie and S. R. Emory, Science **275**, 1102 (1997).
- [7] T. W. Ebbesen *et al.*, Nature (London) **391**, 667 (1998).
- [8] H. J. Lezec *et al.*, Science **297**, 820 (2002).
- [9] A. Degiron *et al.*, Opt. Commun. **239**, 61 (2004).
- [10] D. Magde, E. Elson, and W. W. Webb, Phys. Rev. Lett. **29**, 705 (1972).
- [11] M. J. Levene *et al.*, Science **299**, 682 (2003).
- [12] E. L. Elson and D. Magde, Biopolymers **13**, 1 (1974).
- [13] W. P. Ambrose *et al.*, Science **265**, 364 (1994).
- [14] L. Novotny, Appl. Phys. Lett. **69**, 3806 (1996).
- [15] R. Rigler *et al.*, Eur. Biophys. J. **22**, 169 (1993).
- [16] H. Rigneault and P. F. Lenne, J. Opt. Soc. Am. B **20**, 2203 (2003).
- [17] E. Popov, M. Nevriere, and N. Bonod, J. Opt. Soc. Am. A **21**, 46 (2004).
- [18] N. Bonod, E. Popov, and M. Nevriere, J. Opt. Soc. Am. A **22**, 481 (2005).
- [19] A. R. Zakharian, M. Mansuripur, and J. V. Moloney, Opt. Express **12**, 2631 (2004).
- [20] L. Yin *et al.*, Appl. Phys. Lett. **85**, 467 (2004).